Actin-capping protein promotes microtubule stability by antagonizing the actin activity of mDia1

Francesca Bartolini, Nagendran Ramalingam, and Gregg G. Gundersen
Department of Pathology and Cell Biology, Columbia University, New York, NY 10032

ABSTRACT **In migrating fibroblasts, RhoA and its effector mDia1 regulate the selective stabilization of microtubules (MTs) polarized in the direction of migration. The conserved formin homology 2 domain of mDia1 is involved both in actin polymerization and MT stabilization, and the relationship between these two activities is unknown. We found that latrunculin A (LatA) and jasplakinolide, actin drugs that release mDia1 from actin filament barbed ends, stimulated stable MT formation in serum-starved fibroblasts and caused a redistribution of mDia1 onto MTs. Knockdown of mDia1 by small interfering RNA (siRNA) prevented stable MT induction by LatA, whereas blocking upstream Rho or integrin signaling had no effect. In search of physiological regulators of mDia1, we found that actin-capping protein induced stable MTs in an mDia1-dependent manner and inhibited the translocation of mDia on the ends of growing actin filaments. Knockdown of capping protein by siRNA reduced stable MT levels in proliferating cells and in starved cells stimulated with lysophosphatidic acid. These results show that actin-capping protein is a novel regulator of MT stability that functions by antagonizing mDia1 activity toward actin filaments and suggest a novel form of actin–MT cross-talk in which a single factor acts sequentially on actin and MTs.**

Monitoring Editor
Rong Li
Stowers Institute

Received: May 2, 2012
Revised: Aug 6, 2012
Accepted: Aug 14, 2012

INTRODUCTION

Establishment of polarity in many migrating cells requires the selective capture and stabilization of a subset of microtubules (MTs) oriented toward the leading edge (Gundersen and Bulinski, 1988; Gundersen *et al.*, 2004; Li and Gundersen, 2008). This mechanism ensures that vesicular traffic is spatially biased because the accumulation of posttranslational modifications on these MTs as a result of their longevity (Gundersen *et al.*, 1987; Webster *et al.*, 1987; Khawaja *et al.*, 1988) enhances the interaction of MTs with specific motors and cargoes (Gurland and Gundersen, 1995; Kreitzer *et al.*, 1999; Lin *et al.*, 2002; Reed *et al.*, 2006; Dunn *et al.*, 2008). A distinguishing property of most selectively stabilized MTs is the posttranslational detyrosination of the C-terminal tail of the α-tubulin subunit, which leaves a new C-terminal residue of glutamate exposed. This class of stable MTs has been referred to as Glu MTs to indicate the new C-terminal residue as opposed to dynamic tyrosinated or Tyr MTs (Gundersen *et al.*, 1984). Stable Glu MTs may arise by a capping activity working on the plus ends of the MTs; such MTs neither incorporate nor lose tubulin subunits for extended intervals in vivo (Webster *et al.*, 1987; Infante *et al.*, 2000).

Stable posttranslationally modified MTs are regulated by a RhoA signaling pathway that involves the formin mDia1 and the MT+TIP proteins adenomatous polyposis coli (APC) and EB1 (Cook *et al.*, 1998; Palazzo *et al.*, 2001; Wen *et al.*, 2004; Goulimari *et al.*, 2005). mDia, EB1, and APC bind to one another at independent sites and may form a complex that contributes to capping of the MTs (Wen *et al.*, 2004). mDia1 may also indirectly affect MT stability, as it is necessary for the protein kinase C–dependent phosphorylation of GSK3β, a known negative regulator of MT stability (Eng *et al.*, 2006). Formin homology 2 (FH2)-containing fragments of mDia1, mDia2, and mDia3 also directly bind and stabilize MTs in vitro, and this activity may contribute to their ability to stabilize MTs in cells (Bartolini *et al.*, 2008; Cheng *et al.*, 2011; Gaillard *et al.*, 2011).

This article was published online ahead of print in MBoC in Press (http://www.molbiolcell.org/cgi/doi/10.1091/mbc.E12-05-0338) on August 23, 2012.

Address correspondence to: Gregg G. Gundersen (ggg1@columbia.edu).

Abbreviations used: APC, adenomatous polyposis coli; DAD, diaphanous autoregulatory domain; DID, diaphanous inhibitory domain; DMSO, dimethyl sulfoxide; DP3, FAK reexpressing FAK$^{-/-}$; DRF, diaphanous-related formin; FAK$^{-/-}$, focal adhesion kinase knockout; FH1, formin homology 1; FH2, formin homology 2; FITC, fluorescein isothiocyanate; GAPDH, glyceraldehyde 3-phosphate dehydrogenase; GBD, GTPase binding domain; GFP, green fluorescent protein; IgG, immunoglobulin G; Jasp, jasplakinolide; LatA, latrunculin A; LPA, lysophosphatidic acid; MT, microtubule; PBS, phosphate-buffered saline; PL, poly-lysine; siRNA, small interfering RNA; TIRF, total internal reflection fluorescence; VASP, vasodilator-stimulated phosphoprotein.

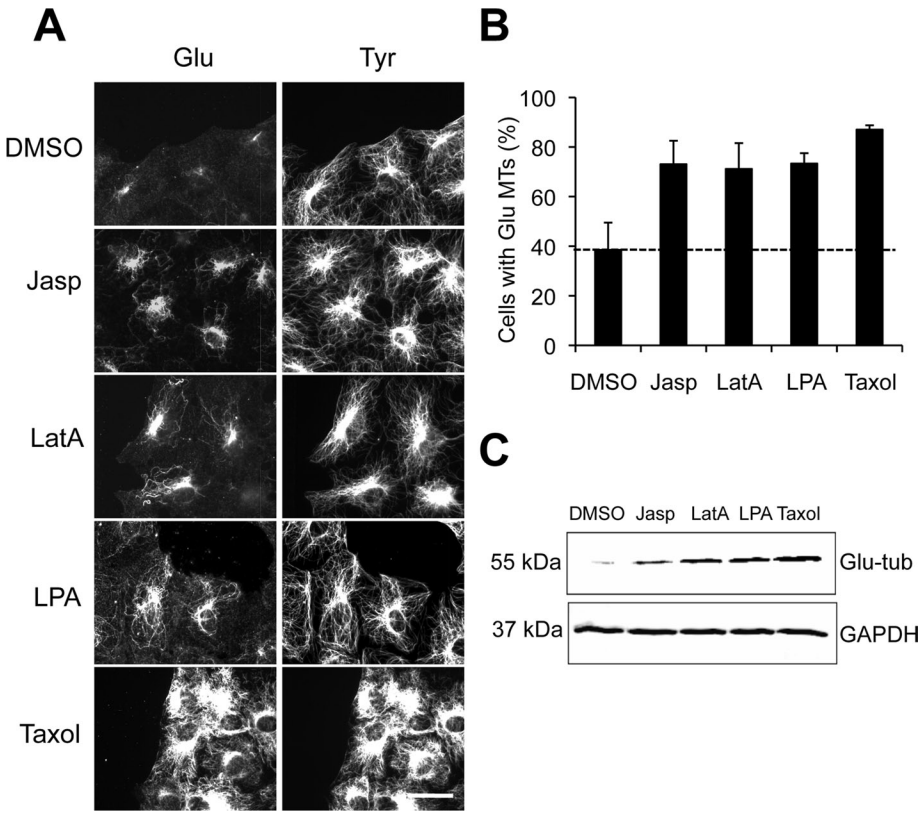

FIGURE 1: Actin drugs induce stable Glu MTs in NIH 3T3 cells. (A) Glu and Tyr tubulin immunostaining of serum-starved NIH 3T3 cells treated with DMSO, 1 μM Jasp, 0.1 μM LatA, 5 μM LPA, or 10 μM Taxol for 1 h before fixation. Scale bar: 20 μm. (B) Quantification of cells treated as in (A) that exhibited >10 Glu MTs (see *Materials and Methods*). Data are mean ± SD from three independent experiments (n >100 cells per experiment). Unstimulated level is shown as a dotted line. (C) Immunoblot analysis of whole-cell lysates from serum-starved NIH 3T3 cells treated with DMSO, 1 μM Jasp, 0.1 μM LatA, 5 μM LPA, or 10 μM Taxol for 2 h prior to lysis. Proteins were resolved by SDS–PAGE and Glu tubulin (Glu-tub) or GAPDH and were detected using specific antibodies.

mDia1 is a diaphanous-related formin (DRF) that nucleates and elongates actin filaments and also promotes the formation of stable Glu MTs. In DRFs, the FH2 domain nucleates and elongates actin filaments at barbed ends in conjunction with the formin homology 1 (FH1) domain, which recruits profilin-bound G-actin (Goode and Eck, 2007). An intramolecular interaction between N-terminus diaphanous inhibitory domain (DID) and C-terminus diaphanous autoregulatory domain (DAD) domains maintains the molecule in an inactive state. The binding of active GTP-Rho to the formin GTPase binding domain (GBD) has been shown to partially unleash this autoinhibition, thus allowing for actin assembly by the FH domains. Release of autoinhibition also appears to regulate MT stabilization, as only expressions of mDia1 and mDia2 fragments lacking the GBD and/or their DAD regions induce MT stability, and expression of the DAD domain alone induces MT stability in serum-starved NIH 3T3 fibroblasts (Palazzo *et al.*, 2001; Wen *et al.*, 2004; Goulimari *et al.*, 2005).

Notably, the actin and MT activities of mDia can be separated. FH2 fragments of mDia2 and mDia3 containing point mutations that prevent stimulation of actin polymerization are still capable of inducing MT stability when introduced into cells (Bartolini *et al.*, 2008; Cheng *et al.*, 2011). The same actin-defective FH2 fragments of both mDia2 and mDia3 retain their ability to bind to MTs, EB1, and APC and generate cold-stable MTs in vitro (Bartolini *et al.*, 2008; Cheng *et al.*, 2011). Hence the FH2 domain of mDia functions in both actin assembly and MT stabilization, suggesting that actin and MTs may compete for this formin in vivo. Molecules that bind to mDia1 may enhance the intrinsic activity of mDia1 toward one of the cytoskeletal elements (Wen *et al.*, 2004; Okada *et al.*, 2010).

We explored the relationship between the actin and MT activities of mDia1 in cells by treating cells with the drugs latrunculin A (LatA) or jasplakinolide (Jasp), which are known to reduce the association of mDia1 with actin filaments. Strikingly, these actin-active drugs induced stable Glu MTs in serum-starved NIH 3T3 cells. We explored the basis for this induction and found that it required mDia1. By testing actin barbed end–interacting proteins, we identified actin-capping protein as a physiological factor that antagonizes mDia1's activity toward actin filaments and enhances its activity toward MTs. Our results identify a new mode of cytoskeletal cross-talk in which a single factor acts sequentially on two cytoskeletal elements.

RESULTS

Actin drugs induce MT stability downstream of Rho and integrin signaling

For testing whether release of mDia1 from actin filaments had an effect on stable MT formation, serum-starved NIH 3T3 cells, which are normally deprived of stable MTs (Gundersen *et al.*, 1994), were incubated with LatA, Jasp, or dimethyl sulfoxide (DMSO) alone for 1 h before analysis of stable MT formation. LatA and Jasp destabilize and stabilize actin filaments, respectively, but both release mDia1 from actin barbed ends (Higashida *et al.*, 2004). Lysophosphatidic acid (LPA), the serum factor responsible for stimulating stable MT formation in fibroblasts (Cook *et al.*, 1998) and Taxol, a drug that stabilizes MTs, were utilized as positive controls. We found that concentrations of LatA and Jasp that affect actin dynamics, but not DMSO alone, induced Glu MTs as assayed immunofluorescently or by Western blot (Figure 1, A–C). Levels of Glu MTs in LatA- or Jasp-treated cells were comparable with those observed in cells treated with the physiological stimulator LPA, but were lower than those observed in cells treated with Taxol, which stabilizes virtually all MTs (Figure 1, A–C). There was no discernible effect of these actin drugs on the overall distribution or levels of dynamic Tyr MTs (Figure 1A and Supplemental Figure S1A). The stability of these de novo–generated Glu MTs was confirmed both by observing their increased levels of acetylation, another posttranslational modification associated with MT longevity, and by their resistance to depolymerization by nocodazole (Figure S1, A–C). These results suggest that actin drugs that release mDia1 from actin filaments induce the formation of a subset of stable, posttranslationally modified MTs.

LatA induction of stable MTs is blocked by dominant-negative EB1 but not upstream inhibitors of the Rho-mDia MT stabilization pathway

As LatA elicited a slightly stronger response in inducing stable Glu MTs than Jasp, we chose to examine its mechanism of action further.

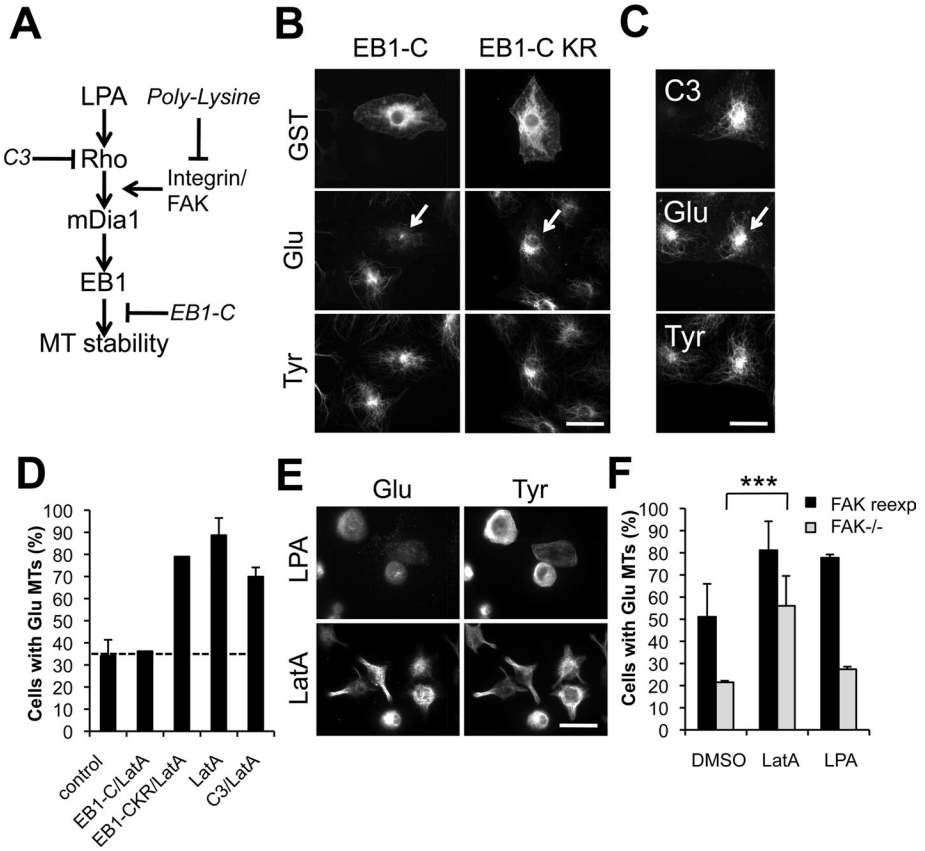

FIGURE 2: Induction of MT stability by actin drugs is downstream of Rho and integrin signaling but upstream of EB1. (A) Schematic of the LPA/Rho/mDia1 pathway leading to MT stabilization. Sites of action of inhibitors (in italics) are indicated by "⊥." (B–D) Immunostaining of GST, human immunoglobulin G (IgG; injection marker for C3), and Glu and Tyr tubulin in serum-starved NIH 3T3 cells injected with GST-EB1-C or GST-EB1-C KR (B) or with C3-toxin plus human IgG (C) before treatment with 0.1 μM LatA for 1 h. Arrows indicate injected cells. (D) Quantification of cells treated as in (B and C) that exhibited >10 Glu MTs. Data are mean ± SD of three independent experiments (n >50 cells per experiment). Uninjected (control) level is shown as a dotted line. (E) Glu and Tyr tubulin immunostaining of NIH 3T3 cells spread on PL before treatment with 5 μM LPA or 0.1 μM LatA for 45 min before fixation. (F) Quantification of serum-starved FAK$^{-/-}$ cells and FAK-reexpressing cells (DP3) that exhibited Glu MTs upon treatment with DMSO, 0.1 μM LatA, or 5 μM LPA for 1 h before fixation. Cells were immunostained for Glu MTs and scored for the presence of > 10 Glu MTs. Data are mean ± SD from three independent experiments (n >100 cells per experiment). ***, p <0.001 calculated by chi-square test. Scale bars for (B), (C), and (E): 20 μm.

As expected, LatA-treated cells had almost no discernible actin stress fibers and partially disrupted cortical actin (Figure S2A). Yet inhibition of myosin or stress fiber formation by myosin II or Rho kinase inhibitors, respectively, did not induce stable Glu MT formation, suggesting that actin-disrupting drugs do not induce MT stability simply by inhibiting myosin contractility or stress fiber formation (Figure S2B).

Given the induction of stable MTs by LatA, we next tested whether LatA functioned within the known Rho/mDia pathway that regulates the selective formation of stable MTs downstream of LPA stimulation (Figure 2A; see Palazzo *et al.*, 2001, 2004; Wen *et al.*, 2004). Initially, we tested inhibitors of the Rho/mDia pathway to determine whether they would block LatA-induced Glu MTs. We analyzed the effects of LatA on MTs in cells microinjected with EB1-C, a C-terminal fragment of EB1 that acts as a dominant negative for Glu MT induction by LPA or active RhoA (Wen *et al.*, 2004), or with botulinin C3 toxin, which specifically inhibits Rho and blocks Glu MT formation induced by LPA (Cook *et al.*, 1998; Figure 2A). C3 toxin had no effect on the induction of Glu MTs by LatA, whereas injection of EB1-C, but not the inactive mutant EB1-C-KR, inhibited the induction of Glu MTs by LatA (Figure 2, B–D). Because RhoA functions upstream of EB1 (Wen *et al.*, 2004), these results suggest that LatA works by stimulating the pathway downstream of RhoA but upstream of EB1.

To further map the level of the pathway at which LatA functioned, we tested whether LatA induced Glu MTs on cells plated on poly-lysine (PL) or in focal adhesion kinase knockout (FAK$^{-/-}$) cells. Integrin signaling through FAK is necessary for RhoA to activate mDia1 but not for artificial activation of mDia1 by DAD expression (Palazzo *et al.*, 2004). Therefore, if LatA induced Glu MTs in cells plated on PL, this would indicate that LatA functioned at the level of mDia1 or downstream of mDia1. LatA induced Glu MTs in wild-type cells plated on PL and in FAK$^{-/-}$ cells, whereas both treatments prevented LPA-induced Glu MTs (Figure 2, E and F). From these results, we conclude that LatA induces MT stability by functioning downstream of RhoA activation and integrin signaling, but upstream of EB1, giving further support to the possibility that a RhoA effector may be responsible for its effect.

LatA induction of stable MTs requires mDia1

In migrating NIH 3T3 fibroblasts, mDia1 is the RhoA effector responsible for inducing the selective stabilization of MTs by LPA (Palazzo *et al.*, 2001; Wen *et al.*, 2004; Eng *et al.*, 2006; Bartolini *et al.*, 2008; Goulimari *et al.*, 2005). To test whether LatA may be stimulating Glu MTs at the level of mDia1, we knocked down mDia1 by injection of specific small interfering RNA (siRNA) oligoduplexes into serum-starved cells before treatment with LatA (Figure 3, A and B). Cells silenced for mDia1 expression, but not control glyceraldehyde 3-phosphate dehydrogenase (GAPDH) expression, failed to generate Glu MTs upon LatA treatment, indicating that mDia1 is required for LatA-induced MT stability. Knockdown of mDia1 by siRNA transfection also reduced LatA-induced Glu tubulin levels, as shown by immunofluorescence and Western blotting (Figure 3, C and D).

To test whether LatA enhanced mDia1 interaction with MTs in cells, we localized mDia1 and MTs before and after LatA treatment. The overall distribution of mDia1 in untreated cells was diffuse, with some enrichment around the nucleus. On LatA treatment, mDia1's distribution became noticeably filamentous and more concentrated near the nucleus, where it overlapped with the focus of the MTs at the centrosome (Figure 4A). At high magnification, more mDia1 puncta appeared colocalized with individual MTs after LatA treatment (Figure 4A). Quantification of mDia1 fluorescence along MTs showed that significantly more mDia1 colocalized with MTs in LatA-treated cells compared with untreated cells (Figure 4B).

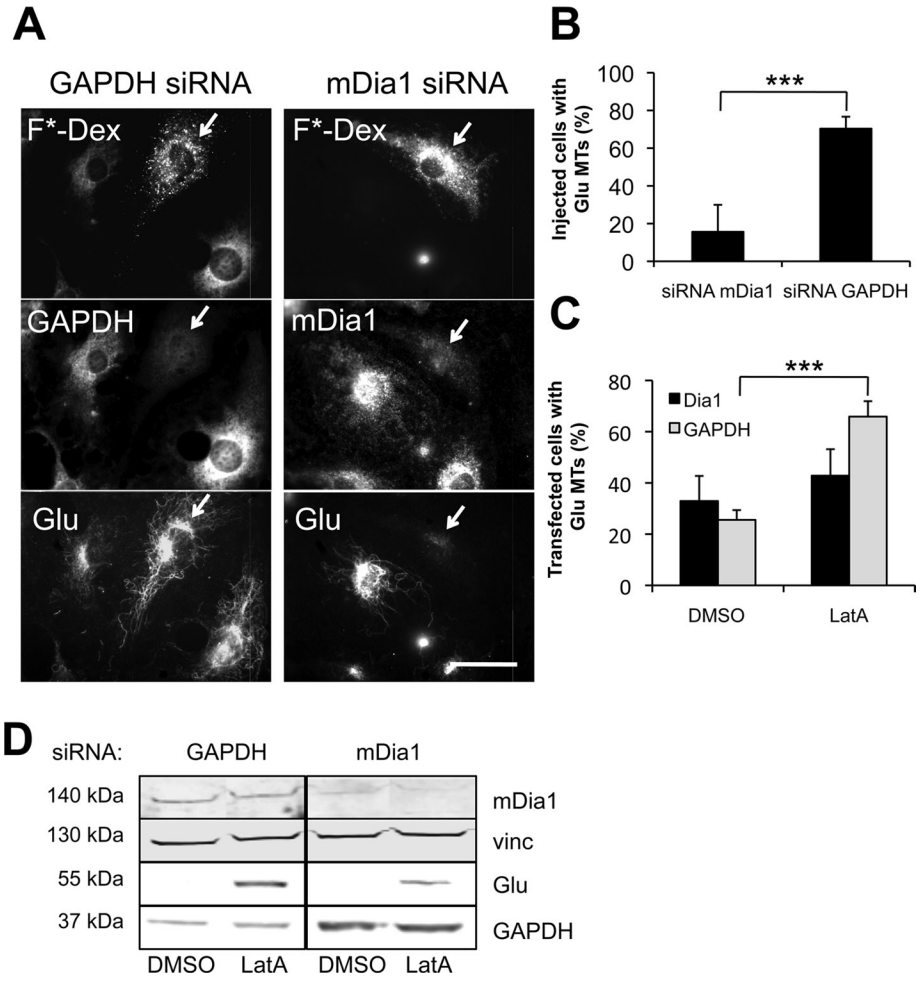

FIGURE 3: Induction of stable Glu MTs by actin drugs requires mDia1. (A) GAPDH, mDia1, and Glu tubulin immunostaining of serum-starved NIH 3T3 fibroblasts injected and incubated for 24 h with GAPDH or mDia1 siRNA before treatment for 1 h with 0.1 μM LatA. siRNA was coinjected with FITC-dextran (F*-Dex) to identify injected cells (arrows). Scale bar: 20 μm. (B) Quantification of cells treated as in (A) that exhibited > 10 Glu MTs. Data are mean ± SD from three experiments (n >100 cells per experiment). ***, p <0.001 calculated by chi-square test. (C) Quantification of NIH 3T3 cells that exhibited > 10 Glu MTs 72-h posttransfection with GAPDH or mDia1 siRNAs. Cells were serum-starved for 48 h the day after transfection and then left untreated or treated with 0.1 μM LatA for 1 h before fixation. Data are mean ± SEM from three experiments (n >100 cells per experiment). ***, p <0.001 calculated by chi-square test. (D) Western blot analysis of whole-cell lysates from cells treated as in (C). GAPDH, mDia1, and Glu tubulin (Glu) levels were detected on the same membrane using specific antibodies. Vinculin (vinc) was used as a loading control.

not fully extend toward the cell periphery, but rather appeared as short filaments clustered around the centrosome. Capping protein expression also increased the percentage of cells that had MTs resistant to nocodazole (42% of cells expressing capping protein vs. 15% of nonexpressing cells), confirming that capping protein induced MT stability (Figure 5C).

In vitro, mDia and capping protein compete for the barbed ends of actin filaments (Goode and Eck, 2007). To test whether capping protein was capable of dislodging mDia from growing barbed ends in cells, we used total internal reflection fluorescence (TIRF) microscopy to examine the directional movement of green fluorescent protein (GFP)-FH1FH2mDia2 puncta, which reflect actin filament elongation (Higashida *et al.*, 2004; Bartolini *et al.*, 2008). We used mDia2 for this experiment because we found that GFP-FH1FH2mDia2 puncta appeared brighter and were easier to trace in NIH 3T3 cells than GFP-FH1FH2mDia1 puncta. As previously observed, GFP-FH1FH2mDia2 puncta moved in a rectilinear manner into the tips of filopodia-like protrusions in control cells injected with injection marker alone (Figure 5D and Supplemental Video S1). In contrast, GFP-FH1FH2mDia2 puncta exhibited virtually no directional movement in cells injected with injection marker and capping protein (Figure 5D and Video S2), indicating that elevated levels of capping protein prevent mDia2 association with actin barbed ends. Capping protein also prevented mDia1 induction of actin filaments in starved cells when coinjected with constitutively active mDia1 (Figure S3).

We tested whether the formation of stable MTs by elevating capping protein levels was mDia1 dependent. In mDia1-depleted cells, injection of capping protein no longer induced formation of Glu MTs (Figure 5, E and F). Localization of mDia1 in cells injected with capping protein revealed colocalization of mDia1 with Glu MTs in ~30% of the injected cells, particularly around the centrosome, where capping protein was mostly concentrated (Figure 5G). These results show that increasing capping protein levels induces stable Glu MTs in an mDia1-dependent manner and that elevated capping protein can induce the redistribution of mDia1 to the MT cytoskeleton. Both of these effects are consistent with the ability of capping protein to reduce mDia1 association with actin barbed ends.

Capping protein regulates Glu MT formation through mDia1

Our results, combined with those of an earlier study that showed mDia1 release upon LatA (Higashida *et al.*, 2004), suggest that reduced association of mDia1 with actin filaments may promote its association with MTs allowing MT stabilization. To further test this idea and examine its possible physiological relevance, we explored whether actin barbed-end binding proteins, which compete with formins, including mDia1, for association with actin filaments (Goode and Eck, 2007), might be involved in MT stabilization. As an initial test of this idea, we expressed capping protein or vasodilator-stimulated phosphoprotein (VASP) in serum-starved cells and assayed induction of Glu MTs (Figure 5). Expression of capping protein, but not VASP, induced the formation of Glu MTs above the levels in nonexpressing cells (Figure 5, A and B). Interestingly, Glu MTs induced by capping protein expression in most of the cells (74%) did

Capping protein, the major high-affinity actin barbed-end terminator in migrating cells, is expressed in all tissues in eukaryotes and is highly enriched in lamellipodia, in which it regulates the length of actin filaments and the transition from filopodia to lamellipodia (Cooper and Pollard, 1985; Cooper and Sept, 2008; Mejillano *et al.*, 2004). To test whether capping protein functioned as a physiological regulator of mDia1 in the formation of Glu MTs, we reduced capping protein levels with two different siRNAs

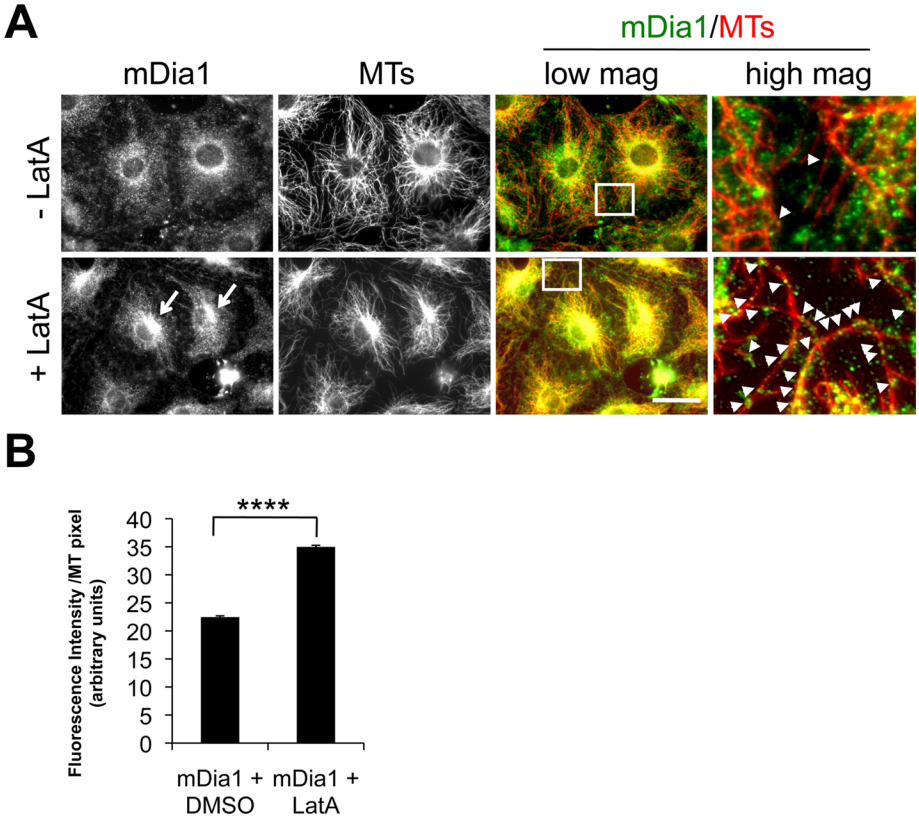

FIGURE 4: LatA induces the colocalization of mDia1 with MTs. (A) mDia1 and Tyr tubulin immunostaining of serum-starved NIH 3T3 cells treated with DMSO or 0.1 μM LatA for 1 h. The far right panels are higher magnifications of the regions shown in the boxes from the low-magnification merged images. Arrows indicate increased mDia1 near the centrosome in LatA-treated cells; arrowheads (in high-magnification merged panels) indicate mDia1 puncta colocalizing with MTs. Scale bar: 20 μm. (B) Quantification of mDia1 fluorescence per MT pixel in cells treated with LatA or DMSO alone. Data are mean ± SEM, and p <0.0001 was obtained by unpaired two-tailed t test.

targeting the ubiquitously expressed β2 subunit of the capping protein αβ heterodimer. As capping protein is an obligate heterodimer, targeting one of the subunits is effective in depleting both (Mejillano *et al.*, 2004), and we observed ~50% knockdown of both subunits with the two siRNAs (Figure 6A). Knocking down capping protein significantly reduced the levels of Glu MTs detected by immunofluorescence in proliferating NIH 3T3 cells compared with controls treated with noncoding siRNA (Figure 6, B and C). Capping protein knockdown also reduced the induction of Glu MTs by LPA in serum-starved NIH 3T3 cells, as assayed by immunofluorescence or by Western blot analysis of Glu tubulin levels (~40% reduction; Figure 6, D and E). Together these results indicate that capping protein plays a physiological role in regulating the levels of Glu MTs.

DISCUSSION

In eukaryotes, the interplay between the actin and MT cytoskeletons is essential for fundamental cellular processes, such as growth, polarity, vesicular transport, and cell division. mDia1 is a RhoA effector that has been implicated both in actin nucleation and polymerization and in MT stabilization downstream of LPA (Goode and Eck, 2007; Bartolini and Gundersen, 2010). Although the two functions are distinct, they both rely on the presence of an intact FH2 domain, suggesting there may be competition between the two cytoskeletal elements in cells.

In this paper, we provide evidence that displacement of mDia1 from actin filaments by capping protein or by actin drugs is sufficient to induce MT stability in serum-starved cells. Induction of MT stabilization by actin disruption was independent of Rho and integrin signaling, while it was substantially reduced in the presence of dominant-negative EB1, which is known to block the effect of LPA and mDia1 on MTs, but not actin remodeling downstream of mDia1 (Figure 2). LatA and capping protein also increased the colocalization of mDia1 with MTs (Figures 4 and 5). These results, coupled with the inability of LatA or capping protein to stimulate MT stabilization in cells depleted of mDia1, strongly suggest that mDia1 mediated the effects of these agents on MTs.

Given that mDia contributes to the formation of actin filaments near the leading edge (Yang *et al.*, 2007), our data suggest a model in which mDia1 released from the actin filaments near the leading edge may stabilize dynamic MTs in the vicinity by binding MTs through association with EB1 and/or through direct interaction with MTs (Figure S4). We propose that capping protein is one of the physiological factors involved in mDia1 release from actin filaments because overexpression of capping protein induced stable MTs in an mDia1-dependent manner, while knockdown reduced stable MT levels in serum-grown cells and in cells stimulated with LPA (Figure 6). Nonetheless, knockdown of capping protein only partially reduced Glu MT levels, which may reflect the incomplete depletion of capping protein we achieved or that additional barbed-end binding proteins contribute to releasing mDia1 so that it can function on MTs. We did not observe induction of Glu MTs upon expression of VASP, but other members of this family, such as Ena or Mena or other proteins affecting actin barbed ends, could be involved. Additional factors may also need to be considered, as recent evidence from studies of yeast formins suggests there are proteins that terminate formin action on actin (Chesarone *et al.*, 2009; Chesarone-Cataldo *et al.*, 2011).

One implication of our model is that some of the mDia1 released from actin would be in an active conformation so that it could interact with MTs in the vicinity. Data to date suggest that the active confirmation of mDia1 for actin filaments and MTs is the same, requiring release of the autoinhibitory DID-DAD interaction (Goode and Eck, 2007; Bartolini and Gundersen, 2010). Thus mDia1 released from actin filaments would be predicted to be in an active conformation with respect to MTs. Active RhoA has been found in the leading edge of cells, and this may contribute to maintaining mDia1 in an active conformation following release from actin filaments. However, this does not explain how LatA and capping protein can stimulate mDia1-dependent MT stabilization in starved cells that have relatively low RhoA GTP levels. Perhaps a local increase in G-actin contributes in these cases; a previous report has implicated G-actin levels in maintaining the activity of mDia1

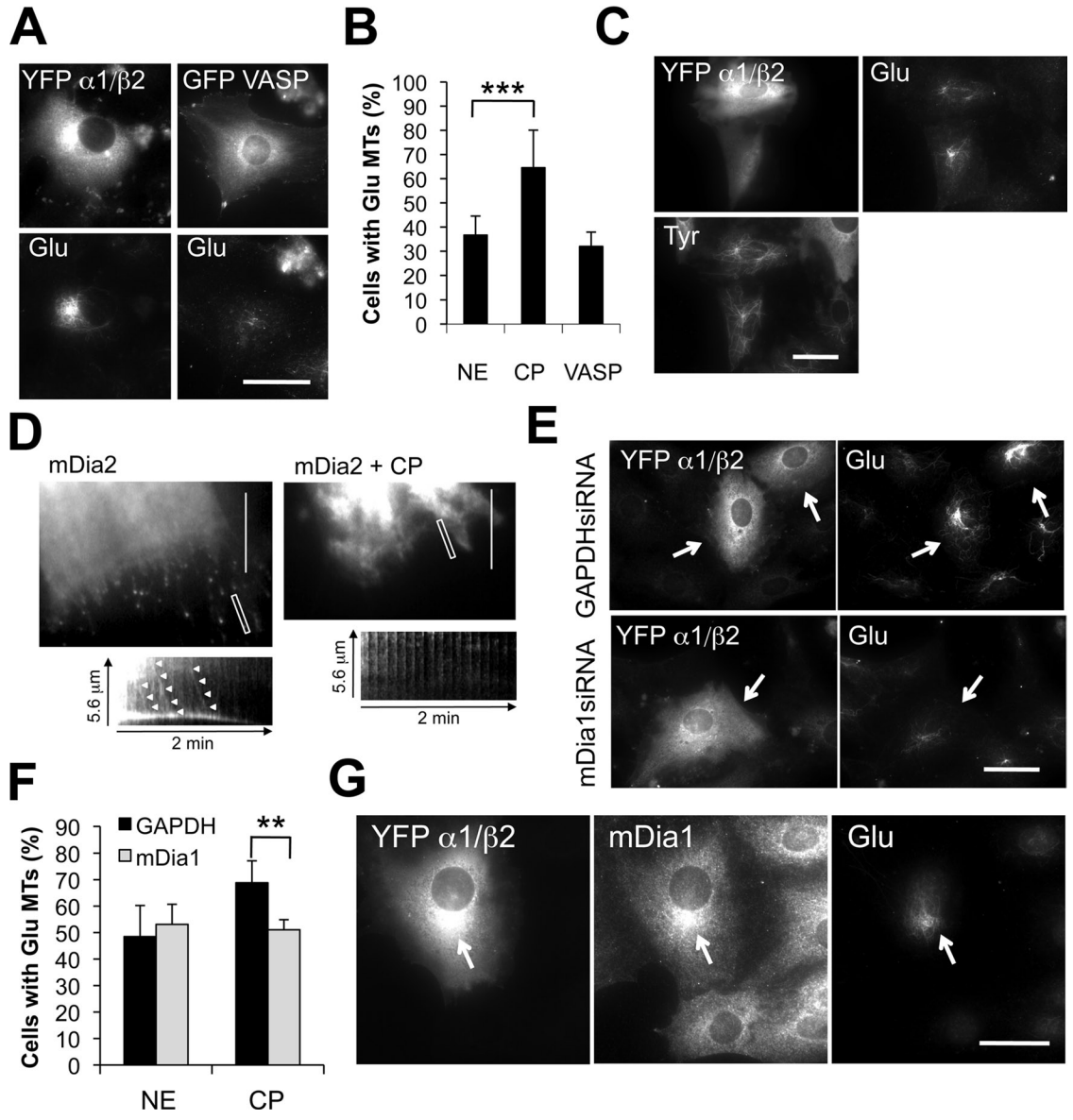

FIGURE 5: Capping protein induces MT stability in an mDia1-dependent manner. (A) Immunostaining of Glu MTs in serum-starved NIH 3T3 cells injected with either YFP-labeled α1/β2 capping protein subunits or GFP-VASP. (B) Quantification of serum-starved cells that exhibited > 10 Glu MTs upon expression of YFP-labeled α1/β2 capping protein (CP) or GFP-VASP. NE, nonexpressing cells. Data are mean ± SD from three experiments (n > 50 cells per experiment). ***, p <0.001 calculated by chi-square test. (C) Immunostaining of Glu and Tyr MTs in NIH 3T3 cells injected with YFP-labeled α1/β2 capping protein and treated with 2 μM nocodazole for 30 min before fixation. (D) TIRF microscopy of GFP-FH1FH2mDia2 puncta in NIH 3T3 cells injected with rhodamine-dextran alone (mDia2) or rhodamine-dextran with His-α1/β2 capping protein (mDia2 + CP). Shown are single frames from representative movies. A kymograph of a selected region (white box) from each movie is shown. Arrowheads indicate moving mDia2 puncta. (E) Immunostaining of Glu MTs in GAPDH or mDia1 siRNA-treated NIH 3T3 cells expressing YFP-labeled α1/β2 capping protein. (F) Quantification of cells treated as in (E) with > 10 Glu MTs. NE, nonexpressing cells. Data are mean ± SD from three experiments (n > 50 cells per experiment). **, p <0.01 by chi-square test. (G) Immunostaining of mDia1 and Glu MTs in an NIH 3T3 cell expressing YFP α1/β2 capping protein. The arrow indicates accumulation of mDia1 near the centrosome in the expressing cell. Scale bars for (A), (C), (E), and (G): 20 μm; (D): 10 μm.

(Higashida *et al.*, 2008), and both LatA and capping protein overexpression would increase G-actin levels. High G-actin levels, such as those near the dynamic actin filaments at the leading edge, may also contribute to physiologically maintaining mDia1 in an active state. Actin perturbation by drugs or capping protein may also enhance the ability of MTs to access the small amount of active mDia1 in the cortex.

The Glu MTs induced by capping protein injection were not extended but rather appeared as a tangle of filaments near the centrosome (Figure 5). We previously observed the same phenotype when actin-inactivating mutants of a minimally active fragment of mDia2 were tested for induction of MT stability (Bartolini *et al.*, 2008). This suggests that interaction of mDia with actin filaments may be required for anchoring or maintaining stabilized MTs at the

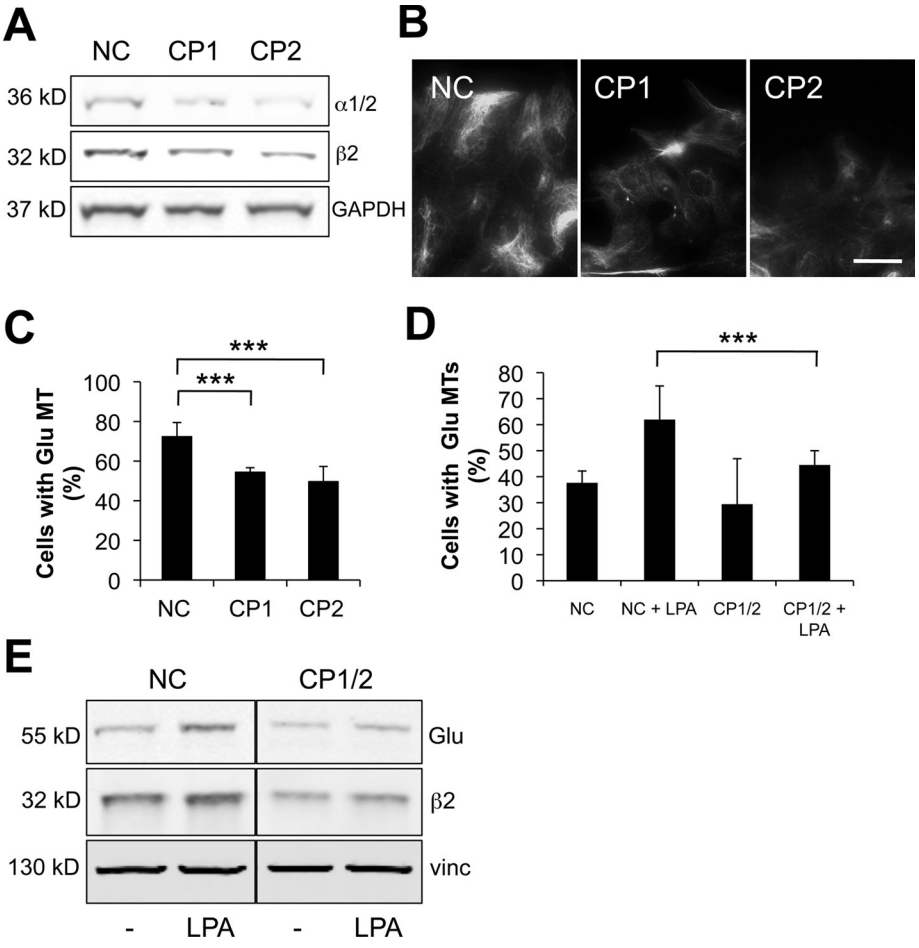

FIGURE 6: Capping protein is required for MT stability. (A) Western blot of proliferating NIH 3T3 cells treated with noncoding siRNA (NC) or distinct capping protein siRNAs (CP1 and CP2). Blots were stained with antibodies to α1/2 or β2 capping protein or GAPDH (as a loading control). (B) Immunostaining of Glu MTs in cells treated with siRNAs as in (A). Scale bar: 20 μm. (C) Quantification of cells treated with siRNAs as in (A and B) that exhibited > 10 Glu MTs (n > 100 per experiment). ***, p <0.001 calculated by chi-square test. (D) Quantification of serum-starved NIH 3T3 cells treated with noncoding (NC) or CP1 and CP2 (CP1/2) siRNAs that exhibited >10 Glu MTs upon stimulation with 2 μM LPA (n > 100 per experiment). ***, p <0.001 calculated by chi-square test. (E) Western blot of serum-starved cells treated with noncoding siRNA (NC) or capping protein siRNAs (CP1 and CP2) before and after stimulation with 1 μM LPA. Blots were stained with antibodies to Glu tubulin, β2 capping protein, or vinculin (as a loading control).

cell periphery. Alternatively, these results may indicate that in the absence of an interaction with actin, the activity of the formin becomes "promiscuous," and rather than being constrained to sites of high concentrations of actin filaments, it is free to stabilize MTs at other sites in the cell.

The model we have proposed, in which there is sequential action of mDia1 on actin filaments and then MTs (Figure S4), helps to explain the observation that stable MTs preferentially form toward the leading edge of migrating cells (Gundersen and Bulinski, 1988). It is worth noting that there are other cases in which there appears to be coordinated action of formins on actin and MTs. During cytokinesis, formins contribute to the formation of the actin contractile ring and may also play a role in stabilizing MTs in the adjacent spindle midzone (Kato *et al.*, 2001; Rundle *et al.*, 2004; Watanabe *et al.*, 2008). In *Drosophila* oocytes, formins regulate actin and MTs during cytoplasmic streaming (Rosales-Nieves *et al.*, 2006). During axon outgrowth, stable MTs form in the proximity of actin filaments in the growth cone, and actin drugs are known to stimulate axon outgrowth and MT stability (Bradke and Dotti, 1999). Interestingly, nanomolar Jasp was recently found to promote stabilization of MTs and extension of projections in detached and circulating tumor cells, and while the mechanism was not studied, this may be another case in which formins may mediate sequential activity on actin and MTs (Balzer *et al.*, 2010). It will be interesting to explore whether the model of sequential action of formins on actin and MTs we propose will apply to these and other cellular activities in which the actin and MT cytoskeletons are coordinated.

Finally, our results showing that drugs whose primary target is the actin cytoskeleton also affect MT stability raise a cautionary note in interpreting the action of these drugs in studies of cells. Secondary consequences of the action of cytoskeletal drugs have been known for some time, with one of the best examples being the activation of Rho GTPase by both actin filament-disruptive (cytochalasin D) and MT-disruptive (nocodazole) drugs (Enomoto, 1996; Ren *et al.*, 1999). Given the myriad interactions of the cytoskeleton with other cellular processes, it is perhaps not surprising that cytoskeletal drugs lead to multiple downstream events, but it will be important to distinguish primary from secondary effects in future studies with these drugs.

MATERIALS AND METHODS

Plasmids and reagents

Construction of pGST-EB1-C and pGST-EB1-C-KR were described previously (Wen *et al.*, 2004). pYFP-capping protein α1 and β2 and capping protein α1/β2::HIS in pRSF-DUET-1 were generously provided by J. Cooper (Washington University, St. Louis, MO). pVASP-GFP and Cherry-FH1-COOH mDia1 were generous gifts from F. B. Gertler (MIT, Cambridge, MA) and B. L. Goode (Brandeis University, Boston, MA), respectively. All chemicals were obtained from Sigma-Aldrich (St. Louis, MO) unless otherwise noted. LPA was purchased from Avanti (Alabaster, AL), and LatA was a gift from P. Crews (University of California, Santa Cruz, CA). Jasp, Y27632, and blebbistatin were purchased from Calbiochem (San Diego, CA). Mouse anti–acetylated tubulin (1:5000, clone 6-11B-1) was from Sigma-Aldrich and rabbit anti–β-catenin (1:250) was from Invitrogen (Carlsbad, CA).

Protein purification

Capping protein α1/β2::HIS in pRSF-DUET-1 was transformed into BL21DE3 cells and the expressed protein was affinity-purified on nickel resin (Clontech, Mountain View, CA) according to the manufacturer's recommended protocols. Purified protein was dialyzed against H-KCl and concentrated using Amicon Ultra-15 (Millipore, Billerica, MA).

Cell culture and microinjection

NIH 3T3 cells were grown in DMEM and 10% calf serum, whereas FAK$^{-/-}$ cells and FAK$^{-/-}$ cells reconstituted with wild-type FAK (DP3) were grown in DMEM plus 10% fetal calf serum, as previously described (Cook *et al.*, 1998; Kreitzer *et al.*, 1999; Palazzo *et al.*, 2001, 2004). For drug and microinjection experiments, cells were grown to confluence on acid-washed coverslips, serum-starved for 48 h, and wounded 30 min before drug or LPA (5 µM) treatment for 1 h or microinjection, as described previously (Cook *et al.*, 1998; Kreitzer *et al.*, 1999; Palazzo *et al.*, 2001). cDNA plasmids were diluted in H-KCl buffer (10 mM HEPES, pH 7.4, and 140 mM KCl) at 50–200 µg/ml, microinjected into nuclei, and allowed to express for 2 h before fixation. siRNA oligoduplexes were diluted in RNAse-free water and injected at 20 µM into 1-d serum-starved cells in combination with the marker fluorescein isothiocyanate (FITC)-dextran (5 mg/ml) 1 d before LatA treatment. Recombinant proteins were microinjected at 2 mg/ml in H-KCl buffer alone or in combination with FITC-dextran, and injected cells were incubated for 2 h before fixation. C3 botulinum toxin (0.1 mg/ml; Cytoskeleton, Denver, CO) was microinjected into cells and after 30 min, cells were treated with LatA for 45 min before fixation. Cells transfected with GFP-FH1FH2mDia2 for 24 h were injected with 200 µM of His-tagged capping protein α1/β2 together with 1 mg/ml of 3 kDa tetramethylrhodamine dextran (Invitrogen) in H-KCl buffer.

Cells spreading assays

Cell spreading assays were as previously described (Palazzo *et al.*, 2004). Briefly, NIH 3T3 cells were detached with trypsin, the trypsin was quenched with soybean trypsin inhibitor (1 mg/ml in phosphate-buffered saline [PBS]), and the cells collected by centrifugation. Cells were washed twice with DMEM with 2% bovine serum albumin and incubated at 37°C in the same medium for 60 min, with the tube rotated every 5 min to prevent cells from clumping. Cells were then plated on coverslips coated with PL (100 µg/ml in PBS) for the indicated times in the presence of either LatA (0.1 µM) or LPA (5 µM) prior to methanol fixation at –20°C for 10 min.

cDNA, siRNA transfection, and Western blot analysis

NIH 3T3 cells were transfected with cDNAs using Lipofectamine Plus (Invitrogen) according to the manufacturer's specifications. siRNA duplexes targeting mDia1 and capping protein β2 were based on previously published sequences (Mejillano *et al.*, 2004; Eng *et al.*, 2006) and were purchased from Shanghai GenePharma and resuspended in RNase-free water at a concentration of 20 µM. The mouse GAPDH siRNA sequence was 5′-AAAGUUGUCAUGGAUGACCTT-3′ and was used as a negative control, as previous experiments showed that knockdown of GAPDH did not affect Glu MT levels (Wen *et al.*, 2004; Eng *et al.*, 2006). NIH 3T3 fibroblasts were transfected with siRNA duplexes using Lipofectamine RNAiMax (Invitrogen) according to the manufacturer's instructions. Knockdown efficiency and effects on Glu MTs formation were analyzed 48 h after transfection. In the LPA stimulation experiments, cells were transfected with siRNA oligoduplexes and 24 h later were serum-starved for 2 d before stimulation. For Western blot analysis, unless stated otherwise, cells were lysed in RIPA buffer (1% TX-100, 50 mM Tris, pH 7.4, 150 mM NaCl, 0.1% SDS, 0.5% Na-deoxycholate, 1 mM phenylmethylsulfonyl fluoride, and protease and phosphatase inhibitors), boiled in Laemmli sample buffer, and separated by SDS–PAGE. Lysate protein concentration was determined by bicinchoninic acid assay and normalized for loading. Antibodies used for blotting were: mouse anti–capping protein α1/α2 subunits (5B12.3) and β2 subunit (3F2.3) (1:1000; Developmental Hybridoma Bank, University of Iowa, Iowa City, IA), mouse anti-mDia1 (clone 51, 1:500; BD Biosciences, San Jose, CA), mouse anti-vinculin (VIN-11-5, 1:5000), rat anti–tyrosinated tubulin (YL-1/2, 1:1000), rabbit anti–Glu tubulin (1:5000; Gundersen *et al.*, 1984), mouse (1:8000) or rabbit (1:1000) anti-GAPDH, mouse anti–β-actin (C4, 1:1000), followed by the appropriate IR680- or IR800-conjugated secondary antibodies (1:5000; Rockland Immunochemicals, Gilbertsville, PA). Quantification was performed with an Odyssey imaging system (LI-COR Biosciences, Lincoln, NE) and digitally processed with Adobe Photoshop (San Jose, CA).

Epifluorescence and TIRF microscopy

In most cases, cells were fixed in methanol at –20°C for 10 min and rehydrated in TBS (10 mM Tris-buffered saline, pH 7.4). Antibodies used for immunostaining were: mouse anti-mDia1 (clone 51, 1:100; BD Transduction), rat anti–tyrosinated tubulin (YL-1/2, 1:10), rabbit anti–Glu tubulin (1:500), mouse anti-GST (1:100; Cell Signaling, Danvers, MA), mouse anti–β-actin (C4, 1:100), mouse anti-GAPDH (1:100), mouse anti–acetylated tubulin (1:100, clone 6-11B-1), followed by the appropriate Cy dye-conjugated secondary antibodies preabsorbed to minimize cross- reaction with other species (Jackson ImmunoResearch, West Grove, PA). For localizing F-actin, cells were fixed in 4% paraformaldehyde for 10 min, permeabilized with 0.5% Triton X-100 for 5 min, and stained with rhodamine-phalloidin (1:500; Invitrogen). Stained samples were observed with a Nikon Optiphot microscope using a 60× Plan-Apochromat objective and filter cubes optimized for coumarin, fluorescein/GFP, rhodamine, and Cy5 fluorescence. Images were acquired with a MicroMax camera (Kodak KAF 1400-chip; Princeton Instruments, Trenton, NJ) using MetaMorph software (MDS Analytical Technologies, Sunnyvale, CA). Cells were scored positive for Glu MTs if > 10 MTs were brightly stained by the Glu antibody. This cutoff for scoring Glu MTs was chosen because serum-starved NIH 3T3 cells generally have fewer than 10 Glu MTs (see Gundersen *et al.*, 1994; Cook *et al.*, 1998; Palazzo *et al.*, 2001). These brightly labeled Glu MTs are clearly distinguishable from the total population of MTs, which contains low levels of Glu tubulin. A minimum of 50–100 cells for each condition were scored per experiment. Data shown are means from at least three independent experiments.

Quantification of mDia1 on MTs

For measuring the intensity of mDia1 fluorescence per MT pixel before and after LatA treatment, a line of 100 pixels was drawn on single MTs near the edge of the cell, and the intensity of mDia1 signal was measured on that line. Line scans of >50 individual MTs per condition were derived using MetaMorph software, and their means were analyzed for statistical significance after background subtraction.

Live-cell imaging by TIRF microscopy

Live-cell imaging of GFP-FH1FH2mDia2 by TIRF microscopy was performed as previously described with a few modifications (Bartolini *et al.*, 2008). Briefly, GFP-FH1FH2mDia2–transfected cells were injected with 200 µM capping protein α1/β2 and injection marker or with injection marker alone. Cells were imaged using MetaMorph software 10 min after injection in recording medium plus 2% calf serum at 37°C. To enhance detection of moving GFP-FH1FH2mDia2 puncta, we background-subtracted each image using an averaged image of the entire image stack of the movie. Kymographs were then generated from the background-subtracted images using selected regions of the cell periphery.

ACKNOWLEDGMENTS

We thank J. Cooper, B. Goode, F. Gertler, and P. Crews for reagents and Sara Nik for excellent technical assistance. We are grateful to the members of the Gundersen lab for critical reading of the manuscript. This work was supported by National Institutes of Health grant GM 62939 to G.G.G.

REFERENCES

Balzer EM, Whipple RA, Cho EH, Matrone MA, Martin SS (2010). Antimitotic chemotherapeutics promote adhesive responses in detached and circulating tumor cells. Breast Cancer Res Treat 121, 65–78.

Bartolini F, Gundersen GG (2010). Formins and microtubules. Biochim Biophys Acta 1803, 164–173.

Bartolini F, Moseley JB, Schmoranzer J, Cassimeris L, Goode BL, Gundersen GG (2008). The formin mDia2 stabilizes microtubules independently of its actin nucleation activity. J Cell Biol 181, 523–536.

Bradke F, Dotti CG (1999). The role of local actin instability in axon formation. Science 283, 1931–1934.

Cheng L, Zhang J, Ahmad S, Rozier L, Yu H, Deng H, Mao Y (2011). Aurora B regulates formin mDia3 in achieving metaphase chromosome alignment. Dev Cell 20, 342–352.

Chesarone M, Gould CJ, Moseley JB, Goode BL (2009). Displacement of formins from growing barbed ends by bud14 is critical for actin cable architecture and function. Dev Cell 16, 292–302.

Chesarone-Cataldo M, Guerin C, Yu JH, Wedlich-Soldner R, Blanchoin L, Goode BL (2011). The myosin passenger protein smy1 controls actin cable structure and dynamics by acting as a formin damper. Dev Cell 21, 217–230.

Cook TA, Nagasaki T, Gundersen GG (1998). Rho guanosine triphosphatase mediates the selective stabilization of microtubules induced by lysophosphatidic acid. J Cell Biol 141, 175–185.

Cooper JA, Pollard TD (1985). Effect of capping protein on the kinetics of actin polymerization. Biochemistry 24, 793–799.

Cooper JA, Sept D (2008). New insights into mechanism and regulation of actin capping protein. Int Rev Cell Mol Biol 267, 183–206.

Dunn S, Morrison EE, Liverpool TB, Molina-Paris C, Cross RA, Alonso MC, Peckham M (2008). Differential trafficking of Kif5c on tyrosinated and detyrosinated microtubules in live cells. J Cell Sci 121, 1085–1095.

Eng CH, Huckaba TM, Gundersen GG (2006). The formin mDia regulates GSK3β through novel PKCs to promote microtubule stabilization but not MTOC reorientation in migrating fibroblasts. Mol Biol Cell 17, 5004–5016.

Enomoto T (1996). Microtubule disruption induces the formation of actin stress fibers and focal adhesions in cultured cells: possible involvement of the rho signal cascade. Cell Struct Funct 21, 317–326.

Gaillard J, Ramabhadran V, Neumanne E, Gurel P, Blanchoin L, Vantard M, Higgs HN (2011). Differential interactions of the formins INF2, mDia1, and mDia2 with microtubules. Mol Biol Cell 22, 4575–4587.

Goode BL, Eck MJ (2007). Mechanism and function of formins in the control of actin assembly. Annu Rev Biochem 76, 593–627.

Goulimari P, Kitzing TM, Knieling H, Brandt DT, Offermanns S, Grosse R (2005). Gα12/13 is essential for directed cell migration and localized Rho-Dia1 function. J Biol Chem 280, 42242–42251.

Gundersen GG, Bulinski JC (1988). Selective stabilization of microtubules oriented toward the direction of cell migration. Proc Natl Acad Sci USA 85, 5946–5950.

Gundersen GG, Gomes ER, Wen Y (2004). Cortical control of microtubule stability and polarization. Curr Opin Cell Biol 16, 106–112.

Gundersen GG, Kalnoski MH, Bulinski JC (1984). Distinct populations of microtubules: tyrosinated and nontyrosinated alpha tubulin are distributed differently in vivo. Cell 38, 779–789.

Gundersen GG, Khawaja S, Bulinski JC (1987). Postpolymerization detyrosination of alpha tubulin: a mechanism for subcellular differentiation of microtubules. J Cell Biol 105, 251–264.

Gundersen GG, Kim I, Chapin CJ (1994). Induction of stable microtubules in 3T3 fibroblasts by TGF-β and serum. J Cell Sci 107, 645–659.

Gurland G, Gundersen GG (1995). Stable, detyrosinated microtubules function to localize vimentin intermediate filaments in fibroblasts. J Cell Biol 131, 1275–1290.

Higashida C, Miyoshi T, Fujita A, Oceguera-Yanez F, Monypenny J, Andou Y, Narumiya S, Watanabe N (2004). Actin polymerization-driven molecular movement of mDia1 in living cells. Science 303, 2007–2010.

Higashida C, Suetsugu S, Tsuji T, Monypenny J, Narumiya S, Watanabe N (2008). G-actin regulates rapid induction of actin nucleation by mDia1 to restore cellular actin polymers. J Cell Sci 121, 3403–3412.

Infante AS, Stein MS, Zhai Y, Borisy GG, Gundersen GG (2000). Detyrosinated (Glu) microtubules are stabilized by an ATP-sensitive plus-end cap. J Cell Sci 113, 3907–3919.

Kato T, Watanabe N, Morishima Y, Fujita A, Ishizaki T, Narumiya S (2001). Localization of a mammalian homolog of diaphanous, mDia1, to the mitotic spindle in HeLa cells. J Cell Sci 114, 775–784.

Khawaja S, Gundersen GG, Bulinski JC (1988). Enhanced stability of microtubules enriched in detyrosinated tubulin is not a direct function of detyrosination level. J Cell Biol 106, 141–149.

Kreitzer G, Liao G, Gundersen GG (1999). Detyrosination of tubulin regulates the interaction of intermediate filaments with microtubules in vivo via a kinesin-dependent mechanism. Mol Biol Cell 10, 1105–1118.

Li R, Gundersen GG (2008). Beyond polymer polarity: how the cytoskeleton builds a polarized cell. Nat Rev Mol Cell Biol 9, 860–873.

Lin SX, Gundersen GG, Maxfield FR (2002). Export from pericentriolar endocytic recycling compartment to cell surface depends on stable, detyrosinated (glu) microtubules and kinesin. Mol Biol Cell 13, 96–109.

Mejillano MR, Kojima S, Applewhite DA, Gertler FB, Svitkina TM, Borisy GG (2004). Lamellipodial versus filopodial mode of the actin nanomachinery: pivotal role of the filament barbed end. Cell 118, 363–373.

Okada K, Bartolini F, Deaconescu AM, Moseley JB, Dogic Z, Grigorieff N, Gundersen GG, Goode BL (2010). Adenomatous polyposis coli protein nucleates actin assembly and synergizes with the formin mDia1. J Cell Biol 189, 1087–1096.

Palazzo AF, Cook TA, Alberts AS, Gundersen GG (2001). mDia mediates Rho-regulated formation and orientation of stable microtubules. Nat Cell Biol 3, 723–729.

Palazzo AF, Eng CH, Schlaepfer DD, Marcantonio EE, Gundersen GG (2004). Localized stabilization of microtubules by integrin- and FAK-facilitated Rho signaling. Science 303, 836–839.

Reed NA, Cai D, Blasius TL, Jih GT, Meyhofer E, Gaertig J, Verhey KJ (2006). Microtubule acetylation promotes kinesin-1 binding and transport. Curr Biol 16, 2166–2172.

Ren XD, Kiosses WB, Schwartz MA (1999). Regulation of the small GTP-binding protein Rho by cell adhesion and the cytoskeleton. EMBO J 18, 578–585.

Rosales-Nieves AE, Johndrow JE, Keller LC, Magie CR, Pinto-Santini DM, Parkhurst SM (2006). Coordination of microtubule and microfilament dynamics by *Drosophila* Rho1, Spire and Cappuccino. Nat Cell Biol 8, 367–376.

Rundle DR, Gorbsky G, Tsiokas L (2004). PKD2 interacts and co-localizes with mDia1 to mitotic spindles of dividing cells: role of mDia1 IN PKD2 localization to mitotic spindles. J Biol Chem 279, 29728–29739.

Watanabe S, Ando Y, Yasuda S, Hosoya H, Watanabe N, Ishizaki T, Narumiya S (2008). mDia2 induces the actin scaffold for the contractile ring and stabilizes its position during cytokinesis in NIH 3T3 cells. Mol Biol Cell 19, 2328–2338.

Webster DR, Gundersen GG, Bulinski JC, Borisy GG (1987). Differential turnover of tyrosinated and detyrosinated microtubules. Proc Natl Acad Sci USA 84, 9040–9044.

Wen Y, Eng CH, Schmoranzer J, Cabrera-Poch N, Morris EJ, Chen M, Wallar BJ, Alberts AS, Gundersen GG (2004). EB1 and APC bind to mDia to stabilize microtubules downstream of Rho and promote cell migration. Nat Cell Biol 6, 820–830.

Yang C, Czech L, Gerboth S, Kojima S, Scita G, Svitkina T (2007). Novel roles of formin mDia2 in lamellipodia and filopodia formation in motile cells. PLoS Biol 5, e317.